Published in final edited form as:
J Pharm Sci. 2008 February ; 97(2): 831–844. doi:10.1002/jps.21003.

Examination of Barriers and Barrier Alteration in Transscleral Iontophoresis

SARAH A. MOLOKHIA[1], **EUN-KEE JEONG**[2], **WILLIAM I. HIGUCHI**[1], and **S. KEVIN LI**[1,3]

1*Pharmaceutics and Pharmaceutical Chemistry, University of Utah, Salt Lake City, Utah 84112*

2*Department of Radiology and Utah Center for Advanced Imaging Research, University of Utah, Salt Lake City, Utah 84108*

3*Division of Pharmaceutical Sciences, College of Pharmacy, University of Cincinnati, Cincinnati, OH 45267*

Abstract

The flux enhancing mechanisms of transscleral iontophoresis are not well understood. The objective of the present study was to investigate the ocular barrier and barrier alterations in transscleral iontophoretic delivery with magnetic resonance imaging (MRI). Experiments involving constant current transscleral iontophoresis of 2 mA (current density 10 mA/cm^2) and subconjunctival injection were conducted with rabbits *in vivo* and postmortem and with excised sclera in side-by-side diffusion cells *in vitro*. The postmortem and *in vitro* experiments were expected to be helpful in clarifying the importance of vascular clearance and other transport barriers in transscleral iontophoresis. Manganese ion (Mn^{2+}) and manganese ethylenediaminetetraacetic acid complex ($MnEDTA^{2-}$) were the model permeants. The results show that pretreatment of the eye with an electric field by iontophoresis enhanced subconjunctival delivery of the permeants to the anterior segment of the eye *in vivo*. This suggests that electric field-induced barrier alterations can be an important absorption enhancing mechanism of ocular iontophoresis. Penetration enhancement was magnified in the postmortem experiments with larger amounts of the permeants delivered into the eye and to the back of the eye. The different results observed in the *in vivo* and postmortem studies can be attributed to ocular clearance in ocular delivery.

Keywords

ocular; iontophoresis; transscleral; drug delivery; MRI

INTRODUCTION

Ocular iontophoresis has been examined for the delivery of drug compounds in the treatments of eye diseases.[1-3] It has been suggested that this technique is relatively safe at low electric current (density)[5-8] and allows drug delivery to the back of the eye.[4-6] In ocular iontophoresis, a donor electrode is placed in the eye and another electrode is placed on another body surface to complete the electrical circuit. The drug to be delivered into the eye is loaded in the donor electrode. An electric field is applied across the eye to enhance the delivery of the drug into the eye. Iontophoresis operates involving the mechanisms of electrophoresis, electroosmosis, and electroporation.[9,10] Electrophoresis is the enhanced movement of an ionic species by an applied electric field.[11] Electroosmosis is the transport of both neutral and charged species by an electric field-induced convective solvent flow.[12,13] Electropermeabilization or

Correspondence to: S. Kevin Li (Telephone: (513) 558-0977; Fax: (513) 558-0978; E-mail: kevin.li@uc.edu).

electroporation is the alteration of the tissue barrier under an electric field; this increases the intrinsic permeability of tissues and enhances transport.[14,15] The mechanisms of electroporation include the formation of aqueous channels in lipid bilayer that can be transient and reversible or irreversible, depending on the magnitude of the applied electric field and the duration of the electric field application.[16,17] The term electroporation is used in this paper to describe any alterations or disruption of the tissue barrier induced by an electric field. Although the mechanisms of iontophoresis have been well characterized in the field of transdermal delivery, the mechanisms of ocular iontophoretic delivery are not well understood. For example, it is well known that electrophoresis is a mechanism of ocular iontophoresis, but iontophoretic delivery of uncharged compounds has been investigated and found to be satisfactory.[3,5] Little is mentioned in the literature about electroosmosis and electroporation in ocular iontophoresis. In a previous study, electroosmotic transport was observed from the anode to cathode during transscleral iontophoresis under physiological pH, suggesting that the sclera is net negatively charged under normal physiological conditions.[10] However, in this study the contribution of transscleral electroosmosis to iontophoretic delivery of small ions was found not to be significant. To understand tissue alteration during ocular iontophoresis, histological and microscopy methods have been employed.[18,19] These methods are suitable to assess gross tissue alteration in the eye caused by iontophoresis. It has been concluded based on these methods that transscleral iontophoresis is not harmful to the tissues at low current densities.[8] Nevertheless, possible barrier alteration of the tissue as a mechanism of iontophoretically enhanced transport has not been fully investigated. This is mainly because histological and microscopy techniques may not be sensitive to study small changes in the tissue barrier resulting from the application of an electric field. It is important to understand such aspects of ocular iontophoresis for the future improvement and utilization of this drug delivery technique.

Previously, it was found that passive transport of Mn^{2+} and of manganese ethylenediaminetetraacetic acid ($MnEDTA^{2-}$) into the eye after subconjunctival injection could not be detected by magnetic resonance imaging (MRI) over a 2 h period after injection *in vivo*.[20] However, when the animals were sacrificed before subconjunctival injection in a postmortem study, significant penetration of Mn^{2+} and $MnEDTA^{2-}$ into the ciliary body, anterior chamber, and posterior chamber near the injection site was observed after the injection, suggesting the importance of a blood vasculature barrier in the subconjunctival route. In these postmortem experiments (i.e., without clearance) ion permeation into the vitreous was still minimal after subconjunctival injection, indicating the existence of a significant tissue barrier such as the retinal epithelial membrane in transscleral transport. Three important questions have been raised. Does electroporation occur during ocular iontophoresis that alters the transscleral tissue barriers such as the retinal epithelium barrier? If iontophoresis alters the tissue barriers, is this effect reversible? What is the role of clearance during iontophoresis and can iontophoresis overcome the clearance barrier to allow better transscleral delivery into the anterior chamber and/or vitreous?

The purpose of the present study was to examine the barriers in transscleral iontophoresis and the effects of iontophoresis upon these barriers. More specifically, the following were to be investigated: (1) the possible role of the electric field in altering tissue barriers during transscleral iontophoresis, and (2) the importance of clearance upon ocular delivery into the eye. To achieve the present objectives, transport experiments were conducted with excised sclera in side-by-side diffusion cells *in vitro* and with rabbits *in vivo* and postmortem. The postmortem studies served as a model to investigate the mechanisms of transscleral iontophoresis without the interference of ocular clearance. MRI was employed in the *in vivo* and postmortem studies because this technique allowed the examination of the distribution of the probe permeants in the eye such as in the vitreous, which would be otherwise difficult to determine in conventional pharmacokinetic studies.

MATERIALS AND METHODS

Strategy

The goal of the present study was to characterize the transscleral barriers during ocular iontophoresis and the effects of iontophoresis upon these barriers. The flux enhancing mechanisms of ocular iontophoresis such as electroporation and their effects on these barriers were to be investigated. Table 1 provides a list of *in vitro*, *in vivo*, and postmortem experiments to be conducted and analyzed in the present study. Experiments A to E were the experiments performed in the present study. Experiments I to IV were from previous studies;[20-22] these results were to be compared with those obtained in the present study. Experiment A was to study possible electric field-induced alteration of the tissue barrier during iontophoresis *in vivo*. Comparison of the results in Experiments A and III would allow the examination of barrier alteration as a possible flux enhancing mechanism in transscleral iontophoresis. Experiment B studied this effect without ocular clearance such as blood vasculature clearance using postmortem rabbits. The results from Experiment B were compared with those from Experiment IV. Experiment E was designed to use an *in vitro* system to quantify the results observed in the *in vivo* and postmortem experiments under similar iontophoresis conditions (Experiments A and B, respectively). The effects of clearance upon ocular delivery to the posterior segment of the eye were assessed by comparing the results in the studies *in vivo* (Experiments I and II) and postmortem (Experiments C and D).

Materials

$MnCl_2$ tetrahydrate was purchased from Spectrum Chemical (Gardena, CA). Ethylenediamine tetraacetic acid (EDTA) and xylazine were purchased from Sigma Chemical (St. Louis, MO). Sodium chloride 0.9% USP (pH between 5 and 7) was from Baxter Healthcare (Deerfield, IL). Ketamine hydrochloride injectable USP (100 mg/ mL) was from Hospira, Inc. (Lake Forest, IL). $Na_2MnEDTA$ solutions (with excess EDTA at 1:1.5 Mn:EDTA ratios) were prepared by the chemicals as received and the pH was adjusted to between 5 and 7 by the addition of concentrated NaOH. ^{3}H-mannitol, ^{14}C-mannitol, and ^{14}C-tetraethyl ammonium (TEA) at >98% purity were purchased from New England Nuclear, PerkinElmer (Boston, MA) and tested for purity using methods specified by the supplier.

For the electrode devices in the *in vivo* and postmortem studies, Silastic® flexible tubing (Tygon, 3/16 I.D. × 5/16 O.D.) was purchased from VWR Scientific (San Francisco, CA). Silver foil (1.5″ × 0.004″) was obtained from EM Science (Gibbstown, NJ). Liquid silver paint was from LADD Research Industries (Williston, VT). The electrode devices were constructed as previously described.[21] Ag was the electrode in the donor chamber in anodal iontophoresis (anode as the donor) and Ag/AgCl was the donor electrode in cathodal iontophoresis (cathode as the donor). Phoresor II Auto constant current iontophoretic device (Model No. 850, Iomed, Inc., Salt Lake City, UT) was the electric current dose controller.

Animals

New Zealand white rabbits of 3–4 kg were purchased from Western Oregon Rabbit Co. (Philomath, OR) for the *in vivo* and postmortem experiments under the approval of the Institutional Animal Care and Use Committee at the University of Utah. The sclera tissues in the present *in vitro* experiments were obtained from both the superior and inferior temporal sections of an excised eye away from the limbus. The enucleated rabbit eyes were obtained from other studies at the University of Utah Animal Resource Center. Briefly, the eye was harvested from the rabbit carcasses immediately after euthanasia and freed from adhering debris such as the conjunctiva and extraocular muscles. A cut was made in the cornea along the limbus and the eye was carefully dissected into two hemispheres with surgical scissors. The vitreous humor was then removed and the sclera–choroid–retina layer was used directly

without choroid and retina removal. Histology was performed on the tissues with Haematoxylin and Eosin (H&E) stain to verify the dissection method.

In Vivo Rabbit Experiments

The *in vivo* study was designed to examine the effect of iontophoresis on the barrier properties of the eye for transscleral delivery (Experiment A). After the rabbits were anesthetized with 25–50 mg/kg ketamine IM and 5–10 mg/kg xylazine IM, an electrode device (diffusion surface area of ~0.2 cm^2) containing only saline was placed on the conjunctiva/sclera near the limbus at the pars plicata/pars plana in the superior cul-de-sac (under the upper eyelid). The return electrode (approximately 4 cm^2 surface area) was placed on a piece of gauze pad (approximately 40 cm^2 surface area) wetted in saline and clamped to the ear on the opposite side of the treated eye. Blank anodal iontophoresis of 2 mA with saline (the pretreatment) was performed for 20 min. Hence, the current density at the surface of the eye was ~10 mA/cm^2 and that across the skin on the ear was ~0.05 mA/cm^2. The applied voltage was generally in the range of 10–20 V the majority of the time in the experiment. Subconjunctival injection of 0.1 mL 40 mM $MnCl_2$ in saline or 0.1 M $MnEDTA^{2-}$ in distilled water was then performed immediately after iontophoresis at the position of the electrode placement. Reversibility of the barrier was examined by subconjunctival injection given at approximately 7 or 30 h after iontophoresis. The delivery and distribution of the probe permeants in the eye were monitored by MRI after subconjunctival injection.

Postmortem Rabbit Experiments

Within 15 min after the rabbits were sacrificed, experiments of subconjunctival injection with iontophoresis pretreatment were conducted (Experiment B). The protocol was similar to that in the *in vivo* experiments. In these experiments, blank 2-mA anodal iontophoresis (iontophoresis with saline) was performed for 20 min on the postmortem rabbits. Immediately following iontophoresis, a subconjunctival injection of 0.1 mL of 40 mM Mn^{2+} was given at the position of the electrode placement. The permeation and distribution of the probe in the eye were then monitored with MRI.

In Experiments C and D, transscleral iontophoresis was performed as described previously.[22] Two different electrode placements were evaluated. An electrode device with 0.4, 4.0, or 40 mM $MnCl_2$ in saline or 0.1 M $Na_2MnEDTA$ in water was placed either on the conjunctiva/sclera at the pars plana next to the limbus (Experiment C) or far away from the limbus near the fornix (Experiment D) in the superior cul-de-sac for transscleral iontophoresis. The position of the electrode was maintained by fixing the wire of the electrode to the MRI coil with adhesive tape and by the pressure from the eyelid. During iontophoresis, the position of the electrode was checked by comparing the relative electrode position to the anatomical structures of the eye in the MR images. The wires to supply the direct current (DC), which ran between the DC current supply device and the electrodes, were twisted and the loop area was minimized to reduce possible noise contribution to MRI. Constant DC of 2 mA, approximately 10 mA/cm^2, was applied to the eye for 20 min. For $MnCl_2$, the donor electrode was the anode. For $Na_2MnEDTA$, the donor electrode was the cathode. The delivery and distribution of the permeants in the eye were monitored by MRI during and after iontophoresis.

Animal MRI and Data Interpretation

Due to the availability of MRI scanners, two MRI systems were used. Unless otherwise stated, animal MRI experiments were carried out with a GE SIGNA 1.5-T (NV/CVi gradient) clinical MRI system (GE Medical System, Inc., Milwaukee, WI) with a temporal mandibular joint coil (TMJ coil: a double surface phased array coil set with 3″ diameter) similar to those described previously.[21] Dynamic MR imaging was performed, with T_1 (spin–lattice relaxation time) weighted spin–echo imaging technique. The imaging parameters were 400 ms TR, 9 ms TE,

256 readout matrix with 160 phase-encoding, and two signal averages to increase signal-to-noise ratio (SNR). Imaging field of view (FOV) was 12 cm in readout direction. Rectangular FOV with 50 or 75% reduction factor was used to reduce the imaging time in phase-encoding direction. The slice thickness was 2 mm with no spacing, resulting in spatial resolution of 0.47 × 0.47 × 2.0 mm^3. Each scan provided at least 10 transaxial image slices to cover the whole eye, but only the images across the center of the eye will be presented in this paper. Prescanning was performed only once for the first data set at the beginning of the experiment, and the imaging parameters included the prescan results, such as transmitter and receiver gains. Imaging time for single time data was approximately 1 min. In the reversibility study—all subconjunctival injections 7 and 30 h after iontophoresis pretreatment and a number of subconjunctival injections immediately after iontophoresis pretreatment for direct comparison—the MRI experiments were conducted with a clinical 3-T MRI system (Trio with Sonata gradient, Siemens Medical Solution, Erlangen, Germany) and a human wrist coil (a transmit/receive volume coil). The imaging parameters were 400 ms TR, 11 ms TE, 256 readout matrix with 192 phase-encoding, and two signal averages. Rectangular FOV of 10 cm in readout direction with 75% reduction factor was used. The slice thickness was 1.0 mm with no spacing. The spatial resolution was 0.4 × 0.4 × 1.0 mm^3. Each scan provided at least twenty transaxial image slices to cover the whole eye. Imaging time for single time data was approximately 2 min. All MRI experiments were carried out at least in triplicate.

In manganese-enhanced MRI, Mn^{2+} ion and $MnEDTA^{2-}$ complex (the model permeants) enhance the relaxivity of the water protons, reduce the proton spin–lattice relaxation times, and enhance the signal in the MR images. The calibration curves of manganese-enhanced signal intensity versus Mn^{2+} and $MnEDTA^{2-}$ concentration at 1.5 T were presented in previous studies.[20,21] According to the data in these studies, the relationships between signal intensity and permeant concentration are parabolic. The very bright voxels (high signal intensities) in aqueous medium and vitreous humor in the MR images represent approximately 0.8 mM Mn^{2+} or 4 mM $MnEDTA^{2-}$. Above and below these concentration levels, the signal intensities gradually declined (darker voxels). Below approximately 0.02 mM Mn^{2+} and 0.1 mM $MnEDTA^{2-}$, there was essentially no signal enhancement. Due to the parabolic behavior, a range of different permeant concentration (e.g., 4.0 and 40 mM $MnCl_2$) was used in the present study to allow MRI data interpretation. In addition, the concentration of the permeants in the tissues and other segments of the eye cannot be evaluated with the present technique because of possible interferences from Mn-tissue binding and the tissue proton relaxation times.[23,24] MR images obtained from the GE system were analyzed with Scion Image program (Scion Corp., Frederick, MD), and Siemens DICOM images were first converted to the analyze format and analyzed using NIH ImageJ. Tissues away from the region of interest (fat tissues behind the eye) were selected and their signals were used as references in the MR images. MR images with tissue reference signals outside the one-standard deviation range of the reference average were not used in the study. The distances between two points or two regions of interest were determined by the number of pixels between the two points in the images.

In Vitro Transport Experiments

The objectives of the *in vitro* transport experiments were to identify possible electric field-induced membrane alteration during iontophoresis and to quantify this effect in an *in vitro* setting. A three-stage protocol (Stages 1, 2, and 3) was employed to examine the effects of the electric fields upon the barrier of excised rabbit sclera tissue. Fresh sclera was prepared from the same day of eye excision in an attempt to preserve the retina. The sclera tissue (with the retina) was sandwiched between the two half-cells of a two-chamber side-by-side diffusion cell with the retina facing the receiver chamber.[10] Each compartment of the diffusion cell has a 2-mL volume and an effective diffusional area of around 0.2 cm^2. The diffusion cell was placed in a circulating water bath at 37 ± 1°C. Saline (2 mL) and donor solution (2 mL) were

pipetted into the receiver and donor chambers, respectively. Trace amounts of radiolabeled TEA and mannitol in saline or 40 mM Mn^{2+} in saline or 0.1 M $MnEDTA^{2-}$ in deionized water was the donor solution. Under the three-stage protocol, Stage 1 was passive transport experiment. Blank anodal iontophoresis of 2 mA was applied for 20 min in Stage 2 with saline in the absence of the permeants in the donor. Phoresor II Auto constant current iontophoretic device (Model No PM 850, Iomed, Inc., Salt Lake City, UT) was the electric current dose controller to provide the electric current. Silver foil and Ag/AgCl coated Ag foil were the conductive elements in the donor and receiver chambers, respectively. Stage 2 was followed by the passive permeability experiment in Stage 3. In the passive transport experiments of Stages 1 and 3, samples were withdrawn from the donor and receiver chambers at predetermined time (30–60 min) intervals. Typically, 20-μL aliquots were taken from the donor chamber, and 1 mL aliquots were withdrawn from the receiver chamber. The same volume of fresh saline was added back to the receiver chamber after each aliquot removal to maintain a constant volume. The duration of the passive transport experiments was 2–3 h, which was at least eight times longer than the transport lag time. The total permeability coefficient (P) of the sclera and retina tissue composite was calculated at steady state under sink conditions (receiver concentrations ≤10% of the donor concentrations):

$$P=\frac{1}{C_D A_D}\frac{\Delta Q}{\Delta t} \quad (1)$$

where C_D is the concentration of the permeant in the donor chamber, A_D is the diffusional surface area, and $\Delta Q/\Delta t$ is the slope of the cumulative amount of the permeant transported across the membrane into the receiver chamber versus time plot. The total permeability coefficient is a function of the permeability coefficient of the sclera–choroid composite and that of the retina:

$$\frac{1}{P}=\frac{1}{P_{\text{retina}}}+\frac{1}{P_{\text{sclera}}} \quad (2)$$

where P_{retina} is the permeability coefficient of the retina, and P_{sclera} is the permeability of the combined sclera and choroid membrane. In the experiments with Mn^{2+} and $MnEDTA^{2-}$, the donor and receiver samples were analyzed by a colorimetric method.[20] In the experiments with radiolabeled permeants, the samples were analyzed using scintillation cocktail (Ultima Gold, Packard Instrument, Meriden, CT) and a liquid scintillation counter (Packard TriCarb Model 1900TR Liquid Scintillation Analyzer).[10] The permeability coefficients of the tissue for the permeants in Stages 1 and 3 were then compared. The *in vitro* study was to mimic the conditions of the *in vivo* and postmortem studies in Experiments A and B for comparison of the *in vitro* results with those obtained *in vivo* and postmortem.

RESULTS

In vivo Rabbit Experiments

Figure 1 is a diagram of an eye to compare with the labeled MR image in Figure 2b. Figure 2 shows the MR images of Experiment A with subconjunctival injection after iontophoresis pretreatment *in vivo*. The MR images of Experiment III in a previous study are also presented in the figure for direct comparison.[20] In this previous study, the anterior chamber, posterior chamber, and vitreous show no sign of the Mn^{2+} and $MnEDTA^{2-}$ (i.e., being below the detection limits) for over 2 h after subconjunctival injection *in vivo* without pretreatment. With iontophoresis pretreatment in the present study, permeants were generally observed to enter the anterior chamber. Rabbit-to-rabbit variability was also observed. Five rabbits in the present Mn^{2+} experiments showed significant permeant penetration as in Figure 2a, and four rabbits showed less penetration enhancement (n = 9). In the $MnEDTA^{2-}$ experiments, all rabbits showed some penetration enhancement as in Figure 2c (n = 3). Possible reasons of the lower signal intensity observed with $MnEDTA^{2-}$ compared to that with Mn^{2+} include the lower

diffusion coefficient of the larger molecular size $MnEDTA^{2-}$ and the weaker MR signal enhancement for $MnEDTA^{2-}$ at the same concentration.[20,21] In general, the effects of penetration enhancement were also observed to decrease over time after iontophoresis in the 7- and 30-h pretreatment experiments, suggesting that these effects were reversible. When subconjunctival injection was given at 7 h after iontophoresis, some penetration enhancement was observed in one rabbit, and little or no enhancement was observed in four rabbits ($n = 5$, data not shown). At 30 h after iontophoresis, the barriers were almost completely recovered as shown by the lack of a significant difference between the electric field pretreated eye and the control without pretreatment ($n = 4$, data not shown).

As an additional note, the results in Experiments A are similar to (but with a slower delivery rate than) those of iontophoresis *in vivo*[22] and subconjunctival injection postmortem.[20] Pretreatment of the eye tissue with an electric field was capable of facilitating permeant diffusion from the subconjunctival space into the anterior chamber. This result suggests that clearance is not the only barrier for transscleral transport *in vivo*. Other tissue barriers may also exist that can be influenced by treatment with an electric field. The alteration of these barriers enhances permeant absorption from the subconjunctival space into the anterior segment of the eye. It was also noted in the MR images (Fig. 2a) that the MR signals of the iris and ciliary body away from subconjunctival depot were enhanced. This finding was confirmed by MRI using a slice orientation that was orthogonal to the transverse orientation normally used in the present study (data not shown). The enhancement of penetration in the iris and ciliary body around the eye, faster than expected from passive diffusion, suggests that pretreatment with an electric field may enhance permeant delivery via local blood circulation in the ciliary body into the anterior chamber.

Postmortem Rabbit Experiments

The MR images of the subconjunctival injection postmortem study with iontophoresis pretreatment (Experiment B, $n = 3$) are presented in Figure 3. The MR images in a previous study (Experiment IV) are also shown in the figure for direct comparison.[20] Compared with the MR images of subconjunctival delivery without pretreatment in this previous study, a larger amount of permeants was observed in the eye. The difference between the subconjunctival results with and without iontophoresis pretreatment again demonstrates the effect of electric field-induced barrier alteration. The enhancement due to the pretreatment was magnified in the rabbit postmortem relative to those *in vivo*. Particularly transport enhancement into the vitreous was observed postmortem. This suggests that the electric field can alter the transscleral barrier to enhance subconjunctival (passive) delivery into the vitreous, in addition to altering the anterior barrier at the ciliary body. This effect could be masked by the effects of clearance *in vivo*, and was only observed in the animal postmortem. The present postmortem result is consistent with the hypothesis that the electric field alters the transscleral tissue barrier, possibly the retinal epithelial membrane.

Figure 4 shows the MR images in the 2-mA iontophoresis study postmortem when the electrode was placed on the sclera next to the limbus (Experiment C). These results show the full extent of the effect of iontophoretic enhanced transport without the interference of clearance and other physiological factors. In the figure, significant amounts of Mn^{2+} and $MnEDTA^{2-}$ were observed to be delivered to the anterior segment of the eye, greater than those observed in the experiment *in vivo*.[22] At the completion of the 20 min iontophoresis, the permeants penetrate as far as 2 mm into the eye from the device/conjunctiva interface. In less than 1 h after iontophoresis, penetration of Mn^{2+} and $MnEDTA^{2-}$ into the ciliary body, anterior chamber, and posterior chamber near the electrode position was observed, especially when a high permeant concentration such as 40 mM Mn^{2+} and 0.1 M $MnEDTA^{2-}$ was used. The permeants continued to diffuse into the posterior segment of the eye after iontophoresis and reached as

far as 5–6 mm into the vitreous from the position of the electrode placement approximately 2 h after iontophoresis. Such permeant diffusion and distribution after iontophoresis were not observed in the *in vivo* experiments[22] when clearance can be a major factor.

Figure 5 presents the MR images after 20-min 2-mA iontophoresis application postmortem with the two different positions of electrode placement in Experiments C and D. Different permeant distributions were observed in the eye when the electrodes were placed at these two positions. The results of 4 mM Mn^{2+} condition are shown in the figure because they provide the most contrast demonstrating the effects of electrode placement. From the MR images in the figure, when the electrode was placed near the limbus, permeants were mainly delivered to the anterior chamber and the anterior parts of the eye. When the electrodes were placed on the sclera away from the limbus towards the fornix, little ion penetration into the anterior chamber was initially observed. In this case, iontophoresis primarily delivered the permeants to the posterior segment of the eye with a larger amount of permeant observed in the posterior segment relative to that in the anterior segment.

In Vitro Results

Table 2 shows the passive permeability results with the sclera (sclera–choroid–retina) in the three stage passive, anodal iontophoresis, and passive experiments *in vitro* (Experiment E). The iontophoresis condition in this experiment was similar to those in the iontophoresis-pretreated subconjunctival injection studies *in vivo* and postmortem (Experiments A and B). The data in Table 2 show no significant difference between the transscleral permeability coefficients in the passive transport runs (Stages 1 and 3) before and after iontophoresis (Stage 2) for TEA, mannitol, Mn^{2+}, and $MnEDTA^{2-}$ ($p > 0.5$ for all permeants). Comparison of the passive permeability coefficients of sclera with retina in the present study to those of sclera without retina in a previous study[20] in an analysis using Eq. 2 allowed the estimation of the permeability coefficients of retina for TEA, mannitol, Mn^{2+}, and $MnEDTA^{2-}$. The permeability coefficients of retina were estimated to be in the order of 5×10^{-5} cm/s for these permeants of small molecular sizes.

DISCUSSION

MRI and Postmortem Model

The present study utilizes the advantages of the noninvasive pharmacokinetic MRI technique and a postmortem model to investigate possible electric field-induced barrier alteration and the effects of clearance upon transscleral delivery during iontophoresis. MRI was employed to examine the distribution of the probe permeants in the eye in transscleral transport with and without the pretreatment of an electric field. The postmortem model provided a method to investigate the properties of the tissue barriers in transscleral iontophoresis without the interference of ocular clearance.[20,25,26] The probe permeants allow the assessment of the ocular barrier with and without iontophoresis (or pretreatment of iontophoresis) for polar and ionic drugs as drug permeation is mainly related to its physicochemical properties such as molecular size, charge, and diffusion coefficient when there is no specific interaction between the drug and ocular tissues. However, caution must be exercised to extrapolate the results of these probe permeants to lipophilic drugs and macromolecules.

Two recent MRI studies have been performed in this laboratory to investigate ocular iontophoresis.[21,22] In a previous study *in vivo*, the transport and distribution of ions into the eye during and after transscleral and transcorneal iontophoresis were compared using MRI.[21] The use of MRI as a technique to evaluate ocular delivery was also discussed. In a subsequent *in vivo* study, the effects of electrode placement, electric current density, and duration of iontophoresis application upon the transscleral transport during and after transscleral

iontophoresis were investigated.[22] The least resistance pathway during transscleral iontophoresis for direct iontophoretically enhanced delivery was determined, and the potential of iontophoresis to directly deliver an ion deep into the vitreous and to the back of the eye was assessed. In a separate study to examine the effect of ocular clearance upon passive transscleral transport, the delivery, and distribution of ions after subconjunctival injection was investigated with MRI utilizing the postmortem model.[20] The present study was designed to address some of the remaining questions such as the effect of ocular clearance upon transscleral iontophoretic transport and possible barrier alteration during iontophoresis. The findings in the present study, which are built upon the data from the previous subconjunctival injection and iontophoresis studies, are now discussed.

Tissue Barrier Alteration: Postmortem and *In vivo* Studies

The 20-min 2-mA iontophoresis conditions employed in the present study were observed to be within human tolerable limits[7] and this electric current level was suggested not to alter the structures of ocular tissues in animals.[8] There was no evidence of gross damage to the general structure of the eye caused by the electrode device with and without the electric current according to the MR images and visual observation of the eye surface in the present *in vivo* and postmortem studies (data not shown). Comparisons of the postmortem results of blank iontophoresis followed by subconjunctival injection (Experiment B) and those of subconjunctival injection without iontophoresis pretreatment[20] (Experiment IV) suggest electric field-induced barrier alteration during ocular iontophoresis. The differences between the *in vivo* results of subconjunctival injection after iontophoresis pretreatment (Experiment A) and subconjunctival injection without pretreatment[20] (Experiment III) are consistent with this assessment. Although the *in vivo* results are more relevant, the postmortem data are more reliable in demonstrating tissue barrier alteration because the postmortem data are not compromised by possible electric field-induced physiological changes that might affect the *in vivo* data. The *in vivo* postmortem data together are evidence of electric field-induced barrier alteration as a flux enhancing mechanism under the conditions of the present transscleral iontophoresis study.

It was suggested in a previous subconjunctival injection study[20] that the least resistive transport pathway in transscleral transport was at the ciliary body, particularly, the pars plana region. This is consistent with the morphology of the ciliary body.[27] The result also suggests the existence of a transscleral barrier hindering the delivery of permeants into the vitreous postmortem. The present study shows that the transscleral barriers can be altered by the electric field during iontophoresis. It is speculated that the retinal epithelial membrane is the barrier[28,29] because the sclera is relatively inert to electric field-induced structure alteration.[10,30] The exact mechanisms of this are not fully understood. For example, electroporation can facilitate transport through the blood vasculature to the anterior chamber by affecting the endothelial cell[31] lining the blood vessels and/or altering the tissue barrier for direct permeation enhancement in the eye. Electric fields can also enhance absorption across retina cell membrane.[32] Further studies are required to determine the actual mechanisms of electroporation in ocular iontophoresis.

It should be noted that the term electroporation is used here to describe the mechanism of enhanced transport due to reversible barrier alterations or disruption induced by an electric field in the present study. This definition is different from the method-related definition which mainly covers the application of short high voltage pulses in transdermal[14] and ocular delivery.[33,34] Under the definition in the present study, electroporation occurs in 20 min 2-mA ocular iontophoresis as evidenced by the increase in transscleral permeation after iontophoresis. Electroporation generally occurs under an electric field of 0.2–1 V per lipid bilayer depending on the composition of the bilayer membrane.[14,17] The exact electrical resistance of the

transscleral barrier and the electrical potential across this barrier during ocular iontophoresis are not available in the present study. If the barrier resistance is greater than 0.1 $k\Omega cm^2$, the current density used in the present study (10 mA/cm^2) will provide an electrical potential greater than 1 V across the barrier. This electrical potential is strong enough to induce cell membrane electroporation, and the mechanism of electroporation in ocular iontophoresis should not be ruled out. Further studies are needed to confirm this hypothesis.

In vitro Transscleral Model

The influence of an electric field on the permeation across the sclera and retina was also investigated *in vitro* (Experiment E). In these experiments, the permeability coefficients of passive transscleral transport before and after the 20 min iontophoresis were determined to be essentially the same, and this contradicts the MR data observed in the postmortem study of blank iontophoresis followed by subconjunctival injection (Experiment B). In the postmortem study, larger amounts of permeants were observed to be delivered into the vitreous when the sclera was pretreated with iontophoresis. The different observations in the *in vitro* and postmortem studies suggest the existence of a transscleral transport barrier in postmortem rabbits that is absent in the side-by-side diffusion cell system *in vitro*, and that this barrier can be altered by the application of the electric field. It is possible that this barrier was compromised during tissue preparation *in vitro*, so the permeability results of the passive transport experiments before and after iontophoresis treatment were not significantly different. This hypothesis is supported by previous data. In previous human retina studies *in vitro* and *in vivo*, the permeability coefficients of retina for FITC-dextrans of low molecular weight were determined to be in the order of 10^{-3} cm/s *in vitro*,[35] but those of retina transport for fluorescein were in the order of 10^{-6} cm/s *in vivo*.[36] The different tissue permeability results in these two previous studies suggest that the retina may be easily compromised in tissue preparation *in vitro*. There may also be other methodology differences in the *in vitro* and *in vivo* studies, resulting in the different permeability values. Hence, the inability of the present *in vitro* method to identify electric field-induced barrier alteration does not seem to be related to the particular *in vitro* methodology employed in the present study but to the general approach of using excised tissue *in vitro* to evaluate transscleral transport in intact eyes.

Effects of Ocular Clearance

To investigate the tissue barrier without the interference of ocular clearance, a postmortem model was utilized. To examine the effects of clearance upon iontophoretic transport using the postmortem data, a main assumption was that the eye tissues such as the choroid, retina, and endothelial cell tight junctions remained functionally and structurally intact postmortem. A previous study suggests that the eye tissues remain viable for several hours postmortem,[25] and a comparison of the MR images *in vivo* and postmortem would allow studying the effects of the blood vasculature barrier and clearance. In the present postmortem study, the results show significantly larger amounts of permeants delivered into the eye compared with those *in vivo*.[22] Deeper penetration of Mn^{2+} into the eye from the iontophoresis application site was observed during iontophoresis. The permeant continued to diffuse into the posterior segment of the eye after iontophoresis and filled more than half of the vitreous, which was not observed *in vivo*. Also noted in the present study was the significant absorption enhancement into the anterior chamber but not into the vitreous in the *in vivo* iontophoresis pretreatment study. This suggests significant clearance toward the back of the eye preventing transscleral penetration *in vivo*. Previous studies have demonstrated the importance of clearance such as blood vasculature clearance in transscleral delivery.[26,29,37] The present results continue to support this hypothesis. The vasculature blood barrier is likely to be related to the choroid.[29] Other factors such as lymphatic clearance [25,26] and elimination via the aqueous humor outflow[38] may also contribute to the differences observed *in vivo* and postmortem. It is also possible that the transscleral barrier is compromised postmortem leading to the larger amount of permeant

delivered into the eye or magnifying the electroporation effect of iontophoresis in the postmortem studies.

Iontophoresis Delivery

The postmortem results can also serve as a baseline model for comparison with a previous *in vivo* iontophoresis study[22] showing the full extent of the effect of iontophoretically enhanced transport without the interference of clearance. A comparison of the extent and penetration depth of permeant delivery in the eye in the present postmortem iontophoresis study (Experiment C) with those after subconjunctival injection in the previous postmortem study[20] clearly demonstrates the effect of the electric field upon drug delivery into the eye over passive diffusion. In addition, the effects of electrode placements upon transscleral delivery during transscleral iontophoresis can also be studied effectively in the postmortem experiments without blood circulation and clearance. A previous study has suggested that the location of electrode placement during ocular iontophoresis affected ocular iontophoretic delivery due to the anatomy of the eye.[22] The anatomical barriers in drug delivery to the anterior segment of the eye are likely to be different from those of the posterior segment.[31] A direct comparison of the penetration pathways of transscleral iontophoresis when the electrode was placed on the sclera near the pars plana (Experiment C) versus that near the fornix (Experiment D) was performed postmortem in the present study. This comparison demonstrates the importance of electrode placement in ocular iontophoresis and supports the previous *in vivo* study conclusion that the lack of posterior iontophoretic delivery with electrode placement near the fornix is related to ocular clearance.[22]

CONCLUSION

The present study demonstrates the utility of the postmortem animal model and MRI in transscleral transport study. In contrast, the transscleral barriers such as the retinal epithelial barrier in the *in vitro* model are believed to be compromised. The present *in vivo* and postmortem results suggest that electroporation (or electropermeabilization) is a flux enhancing mechanism of transscleral iontophoresis. The subconjunctival injection study shows that pretreatment with iontophoresis enhances transscleral delivery to the anterior chamber *in vivo*, which is reversible, and to the posterior segment of the eye postmortem. This is consistent with the hypothesis that the tissue barrier hindering transscleral transport is altered by the electric field during iontophoresis. The data also suggest that clearance such as blood vasculature clearance significantly reduces ocular delivery to the posterior segment of the eye during and after iontophoresis.

ACKNOWLEDGMENTS

This research was supported in part by NIH Grant EY 015181. The authors thank Dr. Paul S. Bernstein for helpful discussion and Anthony L. Tuitupou and Dr. Rajan P. Kochambilli for their help.

REFERENCES

1. Yoo SH, Dursun D, Dubovy S, Miller D, Alfonso E, Forster RK, Behar-Cohen FF, Parel JM. Iontophoresis for the treatment of paecilomyces keratitis. Cornea 2002;21:131–132. [PubMed: 11805526]
2. Eljarrat-Binstock E, Raiskup F, Frucht-Pery J, Domb AJ. Transcorneal and transscleral iontophoresis of dexamethasone phosphate using drug loaded hydrogel. J Control Release 2005;106:386–390. [PubMed: 16026884]
3. Behar-Cohen FF, Parel JM, Pouliquen Y, Thillaye-Goldenberg B, Goureau O, Heydolph S, Courtois Y, De Kozak Y. Iontophoresis of dexamethasone in the treatment of endotoxin-induced-uveitis in rats. Exp Eye Res 1997;65:533–545. [PubMed: 9464186]

4. Lam TT, Edward DP, Zhu XA, Tso MO. Transscleral iontophoresis of dexamethasone. Arch Ophthalmol 1989;107:1368–1371. [PubMed: 2783069]
5. Behar-Cohen FF, El Aouni A, Gautier S, David G, Davis J, Chapon P, Parel JM. Transscleral coulomb-controlled iontophoresis of methylprednisolone into the rabbit eye: Influence of duration of treatment, current intensity, and drug concentration on ocular tissue and fluid levels. Exp Eye Res 2002;74:51–59. [PubMed: 11878818]
6. Voigt M, Kralinger M, Kieselbach G, Chapon P, Anagnoste S, Hayden B, Parel JM. Ocular aspirin distribution: A comparison of intravenous, topical, and coulomb-controlled iontophoresis administration. Invest Ophthalmol Vis Sci 2002;43:3299–3306. [PubMed: 12356838]
7. Parkinson TM, Ferguson E, Febbraro S, Bakhtyari A, King M, Mundasad M. Tolerance of ocular iontophoresis in healthy volunteers. J Ocul Pharmacol Ther 2003;19:145–151. [PubMed: 12804059]
8. Hughes L, Maurice DM. A fresh look at iontophoresis. Arch Ophthalmol 1984;102:1825–1829. [PubMed: 6508622]
9. Eljarrat-Binstock E, Domb AJ. Iontophoresis: A noninvasive ocular drug delivery. J Control Release 2006;110:479–489. [PubMed: 16343678]
10. Li SK, Zhang Y, Zhu H, Higuchi WI, White HS. Influence of asymmetric donor-receiver ion concentration upon transscleral iontophoretic transport. J Pharm Sci 2005;94:847–860. [PubMed: 15736190]
11. Kasting GB. Theoretical models for iontophoretic delivery. Adv Drug Deliv Rev 1992;9:177–199.
12. Peck KD, Srinivasan V, Li SK, Higuchi WI, Ghanem AH. Quantitative description of the effect of molecular size upon electroosmotic flux enhancement during iontophoresis for a synthetic membrane and human epidermal membrane. J Pharm Sci 1996;85:781–788. [PubMed: 8819006]
13. Pikal MJ. The role of electroosmotic flow in transdermal iontophoresis. Adv Drug Del Rev 1992;9:201–237.
14. Chizmadzhev YA, Indenbom AV, Kuzmin PI, Galichenko SV, Weaver JC, Potts RO. Electrical properties of skin at moderate voltages: Contribution of appendageal macropores. Biophys J 1998;74:843–856. [PubMed: 9533696]
15. Li SK, Ghanem A-H, Peck KD, Higuchi WI. Pore induction in human epidermal membrane during low to moderate voltage iontophoresis: A study using AC iontophoresis. J Pharm Sci 1999;88:419–427. [PubMed: 10187752]
16. Glaser RW, Leikin SL, Chernomordik LV, Pastushenko VF, Sokirko AI. Reversible electrical break-down of lipid bilayers: Formation and evolution of pores. Biochim Biophys Acta 1988;940:275–287. [PubMed: 2453213]
17. Chen C, Smye SW, Robinson MP, Evans JA. Membrane electroporation theories: A review. Med Biol Eng Comput 2006;44:5–14. [PubMed: 16929916]
18. Maurice DM. Iontophoresis of fluorescein into the posterior segment of the rabbit eye. Ophthalmology 1986;93:128–132. [PubMed: 3951810]
19. Kralinger MT, Voigt M, Kieselbach GF, Hamasaki D, Hayden BC, Parel JM. Ocular delivery of acetylsalicylic acid by repetitive coulomb-controlled iontophoresis. Ophthalmic Res 2003;35:102–110. [PubMed: 12646751]
20. Li SK, Molokhia SA, Jeong EK. Assessment of subconjunctival delivery with model ionic permeants and magnetic resonance imaging. Pharm Res 2004;21:2175–2184. [PubMed: 15648248]
21. Li SK, Jeong EK, Hastings MS. Magnetic resonance imaging study of current and ion delivery into the eye during transscleral and transcorneal iontophoresis. Invest Ophthalmol Vis Sci 2004;45:1224–1231. [PubMed: 15037591]
22. Molokhia SA, Jeong E-K, Higuchi WI, Li SK. Examination of penetration routes and distribution of ionic permeants during and after transscleral iontophoresis with magnetic resonance imaging. Int J Pharm 2007;335:46–53. [PubMed: 17236728]
23. Spiller M, Brown RD, Koenig SH, Wolf GL. Longitudinal proton relaxation rates in rabbit tissues after intravenous injection of free and chelated Mn^{2+} Magn Reson Med 1988;8:293–313. [PubMed: 2849704]
24. Berkowitz BA, Roberts R, Goebel DJ, Luan H. Noninvasive and simultaneous imaging of layer-specific retinal functional adaptation by manganese-enhanced MRI. Invest Ophthalmol Vis Sci 2006;47:2668–2674. [PubMed: 16723485]

25. Kim H, Robinson MR, Lizak MJ, Tansey G, Lutz RJ, Yuan P, Wang NS, Csaky KG. Controlled drug release from an ocular implant: An evaluation using dynamic three-dimensional magnetic resonance imaging. Invest Ophthalmol Vis Sci 2004;45:2722–2731. [PubMed: 15277497]

26. Robinson MR, Lee SS, Kim H, Kim S, Lutz RJ, Galban C, Bungay PM, Yuan P, Wang NS, Kim J, Csaky KG. A rabbit model for assessing the ocular barriers to the transscleral delivery of triamcinolone acetonide. Exp Eye Res 2006;82:479–487. [PubMed: 16168412]

27. Noske W, Stamm CC, Hirsch M. Tight junctions of the human ciliary epithelium: Regional morphology and implications on transepithelial resistance. Exp Eye Res 1994;59:141–149. [PubMed: 7835403]

28. Cunha-Vaz J. The blood-ocular barriers. Surv Ophthalmol 1979;23:279–296. [PubMed: 380030]

29. Raghava S, Hammond M, Kompella UB. Periocular routes for retinal drug delivery. Expert Opin Drug Deliv 2004;1:99–114. [PubMed: 16296723]

30. Li SK, Zhu H, Higuchi WI. Enhanced transscleral iontophoretic transport with ion-exchange membrane. Pharm Res 2006;23:1857–1867. [PubMed: 16841198]

31. Ghate D, Edelhauser HF. Ocular drug delivery. Expert Opin Drug Deliv 2006;3:275–287. [PubMed: 16506953]

32. Andrieu-Soler C, Doat M, Halhal M, Keller N, Jonet L, BenEzra D, Behar-Cohen F. Enhanced oligonucleotide delivery to mouse retinal cells using iontophoresis. Mol Vis 2006;12:1098–1107. [PubMed: 17093395]

33. Blair-Parks K, Weston BC, Dean DA. High-level gene transfer to the cornea using electroporation. J Gene Med 2002;4:92–100. [PubMed: 11828392]

34. Andrieu-Soler C, Bejjani RA, de Bizemont T, Normand N, BenEzra D, Behar-Cohen F. Ocular gene therapy: A review of nonviral strategies. Mol Vis 2006;12:1334–1347. [PubMed: 17110916]

35. Jackson TL, Antcliff RJ, Hillenkamp J, Marshall J. Human retinal molecular weight exclusion limit and estimate of species variation. Invest Ophthalmol Vis Sci 2003;44:2141–2146. [PubMed: 12714654]

36. Sander B, Larsen M, Moldow B, Lund-Andersen H. Diabetic macular edema: Passive and active transport of fluorescein through the blood-retina barrier. Invest Ophthalmol Vis Sci 2001;42:433–438. [PubMed: 11157879]

37. Lee TW, Robinson JR. Drug delivery to the posterior segment of the eye II: Development and validation of a simple pharmacokinetic model for subconjunctival injection. J Ocul Pharmacol Ther 2004;20:43–53. [PubMed: 15006158]

38. Wu JC, Jesmanowicz A, Hyde JS. Anterior segment high resolution MRI: Aqueous humor dynamics observed using contrast agents. Exp Eye Res 1992;54:145–148. [PubMed: 1541333]

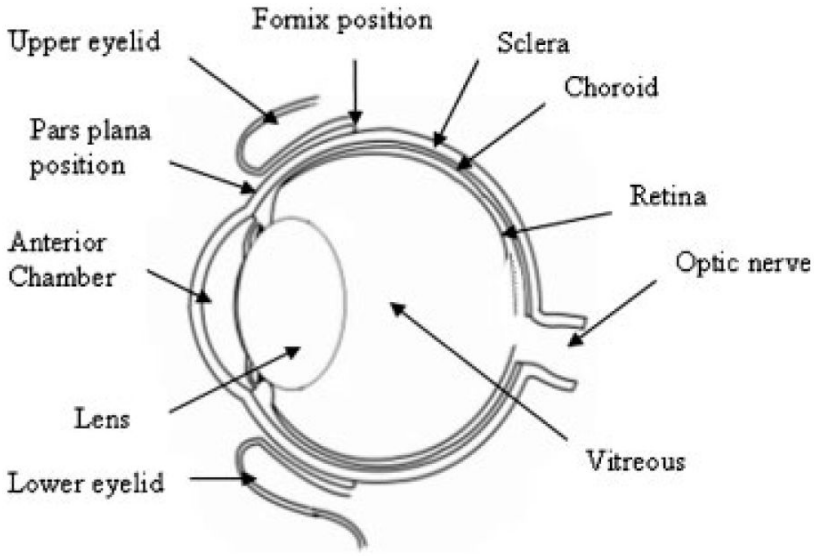

Figure 1.
Rabbit eye diagram.

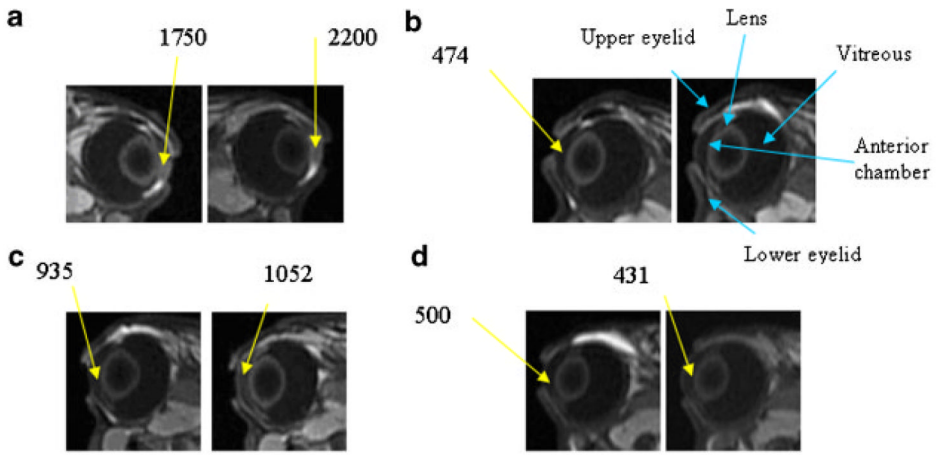

Figure 2.

Representative MR images of *in vivo* studies in Experiments A (blank iontophoresis of 2 mA followed by 0.1 mL subconjunctival injection) and Experiment III (0.1 mL subconjunctival injection without iontophoresis pretreatment). a: Experiment A, injection of 40 mM Mn^{2+} showing significant penetration enhancement, (b) Experiment III, injection of 40 mM Mn^{2+}, (c) Experiment A, injection of 0.1 M $MnEDTA^{2-}$ showing some penetration enhancement, and (d) Experiment III, injection of 0.1 M $MnEDTA^{2-}$. From left to right, images obtained at (a) 40 and 70 min, (b) 30 and 138 min, (c) 21 and 124 min, and (d) 40 and 120 min after injection, respectively. Images in (b) and (d) are obtained from a previous study.[20] The numbers indicate the MR signals from the region of interest (average of 9 voxels or 4 mm^3). The orientations of the eyes in the images (facing left or right) denote the left or right eye.

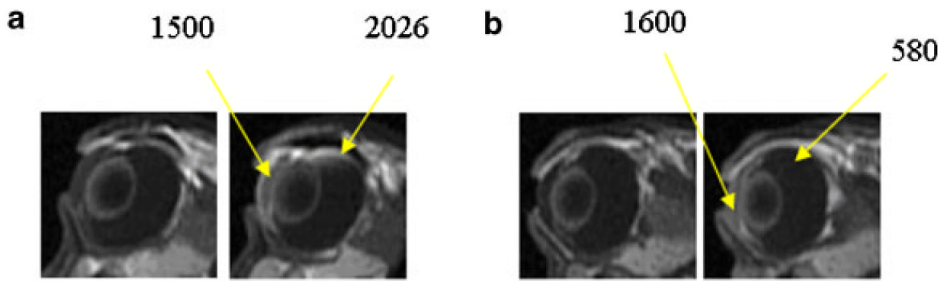

Figure 3.
Representative MR images of postmortem studies in (a) Experiment B, blank iontophoresis of 2 mA followed by 0.1 mL subconjunctival injection of 40 mM Mn^{2+} and (b) Experiment IV, 0.1 mL subconjunctival injection of 40 mM Mn^{2+}. From left to right, for (a) and (b), images obtained at 30 and 60 min after injection. Images in (b) are obtained from a previous study.[20] The numbers indicate the MR signals from the region of interest (average of 9 voxels or 4 mm^3).

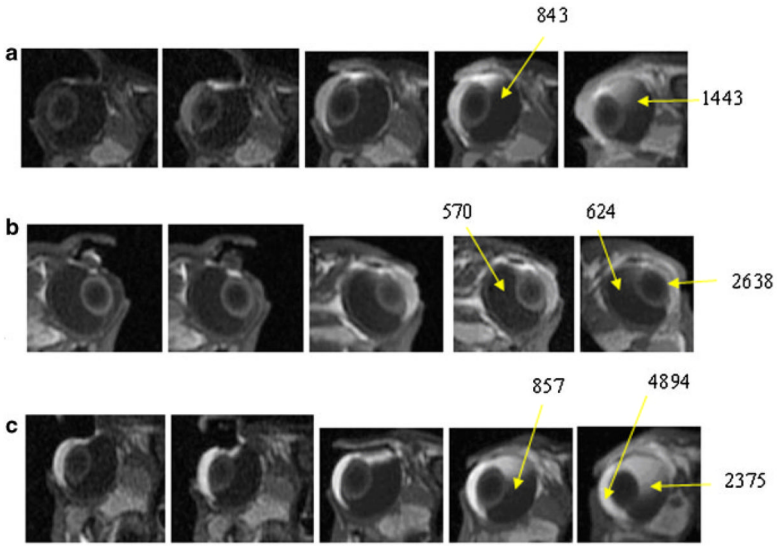

Figure 4.

Representative MR images of postmortem transscleral iontophoresis experiment of 2 mA of (a) 0.1 M $MnEDTA^{2-}$, (b) 4 mM Mn^{2+}, and (c) 40 mM Mn^{2+} in Experiment C. From left to right, images obtained at (a) 9 and 19 min during iontophoresis, and 10, 55 and 140 min after iontophoresis, (b) 10 and 19 min during iontophoresis, and 40, 60, and 190 min after iontophoresis, and (c) 9 and 18 min during iontophoresis, and 10, 60, and 140 min after iontophoresis. Note that high Mn^{2+} and $MnEDTA^{2-}$ concentrations such as 40 mM Mn^{2+} and 0.1 M $MnEDTA^{2-}$ in the electrode device are represented by dark voxels in the images due to the parabolic signal versus concentration relationship. The numbers indicate the MR signals from the region of interest (average of 9 voxels or 4 mm^3).

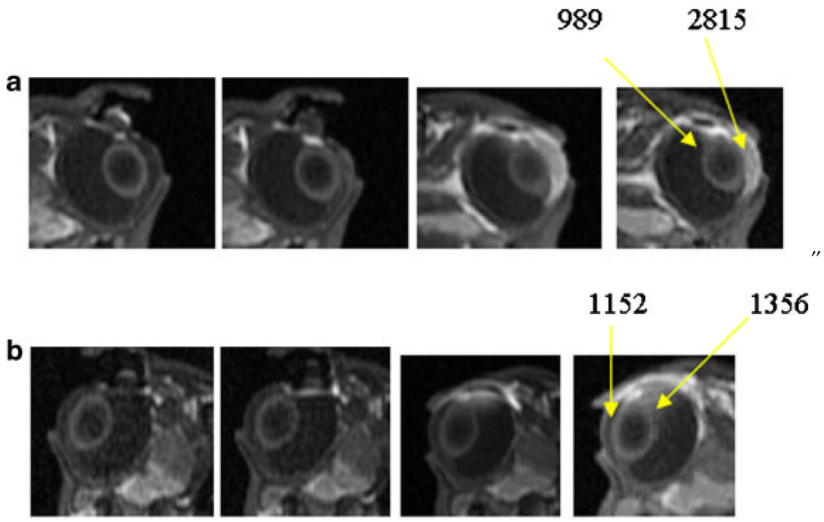

Figure 5.

Representative MR images of postmortem transscleral iontophoresis of 4 mM Mn^{2+} and 2 mA postmortem in Experiments C and D. From left to right, images obtained at (a) 10 and 19 min during iontophoresis, and 40 and 60 min after iontophoresis, with electrode at the pars plana and (b) 11 and 20 min during iontophoresis, and 40 and 86 min after iontophoresis, with electrode at the back of the eye near the fornix. The numbers indicate the MR signals from the region of interest (average of 9 voxels or 4 mm^3).

Table 1

Summary of Experiments Conducted and Analyzed in the Present Study

Experiment	System	Procedure
A	In vivo	Iontophoresis pretreated subconjunctival injection
I	In vivo	Transscleral iontophoresis near limbus, 2 mA, 20 min[a]
II	In vivo	Transscleral iontophoresis near fornix, 2 mA, 20 min[a]
III	In vivo	Subconjunctival injection[b]
B	Postmortem	Iontophoresis pretreated subconjunctival injection
C	Postmortem	Transscleral iontophoresis near limbus, 2 mA, 20 min
D	Postmortem	Transscleral iontophoresis near fornix, 2 mA, 20 min
IV	Postmortem	Subconjunctival injection[b]
E	In vitro	Reversibility/iontophoresis pretreated passive

[a] From Reference [22].

[b] From Reference [20].

Table 2

Permeability Coefficients of Passive Transscleral Transport Before and After Iontophoresis Treatment (Experiment E) [a]

	Permeability Coefficient Before Iontophoresis, P_1 (10^{-5} cm/s)	Permeability Coefficient After Iontophoresis Pretreatment, P_3 (10^{-5} cm/s)	Ratio P_1/P_3
TEA	2.3±1.2	2.6±1.0	0.9±0.2
Mannitol	1.7±0.9	1.9±0.9	0.9±0.1
40 mM Mn^{2+}	1.5±0.5	1.7±0.5	0.9±0.1
0.1 M $MnEDTA^{2-}$	1.4±0.4	1.5±0.2	0.9±0.2

[a] Mean±SD ($n \geq 3$).